THE ASTROPHYSICAL JOURNAL, 430:839–849, 1994 August 1

WHOLE EARTH TELESCOPE OBSERVATIONS OF THE DBV WHITE DWARF GD 358

D. E. WINGET,[1] R. E. NATHER,[1] J. C. CLEMENS,[1] J. L. PROVENCAL,[1] S. J. KLEINMAN,[1] P. A. BRADLEY,[1,2]
C. F. CLAVER,[1,3] J. S. DIXSON,[1] M. H. MONTGOMERY,[1] C. J. HANSEN,[4] B. P. HINE,[5] P. BIRCH,[6] M. CANDY,[6]
T. M. K. MARAR,[7] S. SEETHA,[7] B. N. ASHOKA,[7] E. M. LEIBOWITZ,[8] D. O'DONOGHUE,[9] B. WARNER,[9]
D. A. H. BUCKLEY,[9] P. TRIPE,[9] G. VAUCLAIR,[10] N. DOLEZ,[10] M. CHEVRETON,[11] T. SERRE,[11]
R. GARRIDO,[12] S. O. KEPLER,[13,14] A. KANAAN,[13] T. AUGUSTEIJN,[15] M. A. WOOD,[16]
P. BERGERON,[17] AND A. D. GRAUER[18,19]
Received 1993 September 16; accepted 1994 January 28

ABSTRACT

We report on the analysis of 154 hours of early continuous high-speed photometry on the pulsating DB white dwarf (DBV) GD 358, obtained during the Whole Earth Telescope (WET) run of 1990 May. The power spectrum of the light curve is dominated by power in the range from 1000 to 2400 μHz, with more than 180 significant peaks in the total spectrum. We identify all of the triplet frequencies as degree $\ell = 1$, and from the details of their spacings we derive the total stellar mass as $0.61 \pm 0.03\ M_{\odot}$, the mass of the outer helium envelope as $2.0 \pm 1.0 \times 10^{-6}\ M_{*}$, the absolute luminosity as $0.050 \pm 0.012\ L_{\odot}$ and the distance as 42 ± 3 pc. We find strong evidence for differential rotation in the radial direction—the outer envelope is rotating at least 1.8 times faster than the core—and we detect the presence of a weak magnetic field with a strength of 1300 ± 300 G. We also find a significant power at the sums and differences of the dominant frequencies, indicating nonlinear processes are significant, but they have a richness and complexity that rules out resonant mode coupling as a major cause.

Subject headings: stars: individual (GD 358) — stars: oscillations — white dwarfs

1. INTRODUCTION

The asteroseismology of stellar remnants (e.g., white dwarfs) can provide new and important constraints on our models for the evolution of stars, and can help unravel the history of our Galaxy—how long ago stars first began to form, and how they differed from those now forming. We apply this technique to the variable white dwarf stars by recording their rapid luminosity variations, using a network of photometric telescopes at different longitudes to minimize gaps in the observational coverage. We refer to this network as the Whole Earth Telescope (WET). Our methods of data acquisitions and reduction are described in Nather et al. (1990), and our methods of analysis in Winget et al. (1991).

Only a few of the known white dwarfs are luminosity variables—those with surface temperatures that yield maximum opacity for their atmospheric compositions—but they are otherwise normal white dwarfs (McGraw 1977; Winget 1988) and therefore are good representatives of the white dwarf population in general. If we accept the age of the Galaxy derived from the white dwarf luminosity function (Winget et al. 1987; Wood 1992) and the length of time stars of differing masses spend on the main sequence from evolutionary stellar models (e.g., Iben & Renzini 1983), we must conclude that the current population of white dwarfs in the Galactic disk has been formed entirely from stars more massive than the Sun. Their present internal composition, established when their burnable fuel was exhausted, has been modified only by the benign processes of gravitational contraction, chemical diffusion, and secular cooling. We can therefore hope to reconstruct their prior history from knowledge of their current interiors, which we extract from the analysis of their photometric variations.

We report here the first asteroseismological analysis of a DBV (helium atmosphere) white dwarf, GD 358 (V777 Her, WD 1645+325) and compare it with our earlier results on the hot DOV pre–white dwarf PG 1159−035.

2. THE OBSERVATIONS

GD 358 ($\alpha = 16^{h}47^{m}18^{s}$, $\delta = +32°28'24''$(2000)), the brightest known DB variable with a visual magnitude of 13.7, was the primary WET target in 1990 May. Our data were obtained by combining a total of 48 individual runs, spanning 11 days, from observatories well distributed around the globe (Table 1),

[1] Department of Astronomy and McDonald Observatory, University of Texas, Austin, TX 78712.
[2] Current address: X-2 Division, MS B-220, Los Alamos National Laboratory, Los Alamos, NM 87545.
[3] Visiting Astronomer, Institute for Astronomy, Honolulu, HI.
[4] JILA, University of Colorado, Box 448, Boulder CO 80309.
[5] NASA Ames Research Center, M.S. 44-4, Moffett Field, CA 94035.
[6] Perth Observatory, Bickley, Western Australia.
[7] Indian Space Research Organization, Technical Physics Division, ISRO Satellite Centre, Airport Rd., Bangalore 560 017, India.
[8] Department of Physics and Astronomy, University of Tel Aviv, Ramat Aviv, Tel Aviv 69978, Israel.
[9] Department of Astronomy, University of Cape Town, Rondebosch 7700, Cape Province, South Africa.
[10] Observatoire Midi-Pyrenees, 14 Avenue E. Belin, 31400 Toulouse, France.
[11] Observatoire de Paris-Meudon, F-9195 Meudon Principal Cedex, France.
[12] Instituto de Astrofisica de Andalucia, Granada, Spain.
[13] Instituto de Fisica, Universidade Federal do Rio Grande do Sul, 90049 Porto Alegre RS, Brazil.
[14] Visiting Astronomer, Cerro Tololo Interamerican Observatory.
[15] European Southern Observatory, La Silla, Chile.
[16] Department of Physics and Space Sciences, Florida Institute of Technology, 150 W. University Blvd., Melbourne, FL 32901.
[17] Département de Physique, Université de Montréal, C.P. 6128, Succ. A, Montréal, Québec, Canada H3C 3J7.
[18] Department of Physics and Astronomy, University of Arkansas at Little Rock, 801 S. University Av., Little Rock, AR 72204.
[19] Visiting Astronomer, Kitt Peak National Observatory.

TABLE 1

JOURNAL OF OBSERVATIONS

Run Name	Telescope	Date (UT)	Start Time (UTC)	Run Length (s)
cfc-0034	Mauna Kea 24″	1990 May 20	6:26:30	21800
jcc-0145	Perth 24″	1990 May 20	14:33:00	11700
ra138	Itajuba 1.60 m	1990 May 21	1:10:40	10750
sjk-0080	ESO 1.0 m	1990 May 21	3:31:30	4970
sjk-0081	ESO 1.0 m	1990 May 21	5:00:30	1240
sjk-0082	ESO 1.0 m	1990 May 21	5:50:00	3770
cfc-0035	Mauna Kea 24″	1990 May 21	6:16:00	26660
sjk-0083	ESO 1.0 m	1990 May 21	7:08:00	5300
jcc-0147	Perth 24″	1990 May 21	14:12:30	21760
sjk-0086	ESO 1.0 m	1990 May 22	2:59:30	19910
pab-0038	McDonald 0.9 m	1990 May 22	4:22:00	9270
jcc-0150	Perth 24″	1990 May 22	14:10:00	21420
eml-011	Wise 40″	1990 May 22	19:22:01	21960
s5084	SAAO 0.75 m	1990 May 22	20:52:00	13210
ra144	Itajuba 1.6 m	1990 May 23	1:55:52	3310
sjk-0089	ESO 1.0 m	1990 May 23	2:56:30	19960
ra145	Itajuba 1.6 m	1990 May 23	3:23:22	5810
ra146	Itajuba 1.6 m	1990 May 23	5:01:10	7560
cfc-0037	Mauna Kea 24″	1990 May 23	6:00:00	4100
cfc-0038	Mauna Kea 24″	1990 May 23	7:10:10	10720
a230	Kitt Peak 50″	1990 May 23	8:27:00	9860
cfc-0040	Mauna Kea 24″	1990 May 23	11:09:20	1090
cfc-0037	Mauna Kea 24″	1990 May 23	11:33:20	2370
cfc-0038	Mauna Kea 24″	1990 May 23	12:35:10	4260
jcc-0153	Perth 24″	1990 May 23	14:18:30	20620
eml-022	Wise 40″	1990 May 23	18:57:31	23690
ra152	Itajuba 1.6 m	1990 May 24	1:08:20	13790
ra153	Itajuba 1.6 m	1990 May 24	5:00:10	6290
cfc-0039	Mauna Kea 24″	1990 May 24	10:00:00	10750
cfc-0040	Mauna Kea 24″	1990 May 24	13:13:40	4970
eml-033	Wise 40″	1990 May 24	19:19:51	22060
ra156	Itajuba 1.6 m	1990 May 25	1:11:30	12700
pab-0039	McDonald 0.9 m	1990 May 25	4:31:00	6010
ra157	Itajuba 1.6 m	1990 May 25	5:31:50	7580
cfc-0039	Mauna Kea 24″	1990 May 25	6:00:00	28510
eml-045	Wise 40″	1990 May 25	19:15:01	22320
ra160	Itajuba 1.6 m	1990 May 26	1:05:20	8630
pab-0040	McDonald 0.9 m	1990 May 26	3:20:00	11330
ra161	Itajuba 1.6 m	1990 May 26	3:36:40	12400
a234	Ktt Peak 50″	1990 May 26	4:48:00	11690
cfc-0046	Mauna Kea 24″	1990 May 26	6:00:00	2710
cfc-0047	Mauna Kea 24″	1990 May 26	7:43:10	17770
eml-058	Wise 40″	1990 May 26	19:06:41	22720
pab-0042	McDonald 0.9 m	1990 May 27	3:01:00	27000
sjk-0091	ESO 1.0 m	1990 May 27	4:10:30	1410
cfc-0050	Mauna Kea 24″	1990 May 27	13:04:30	5300
eml-069	Wise 40″	1990 May 27	19:01:01	22980
eml-080	Wise 40″	1990 May 28	19:08:41	22400
pab-0045	McDonald 0.9 m	1990 May 29	5:33:00	3980
pab-0047	McDonald 0.9 m	1990 May 30	6:53:30	13530
pab-0048	McDonald 0.9 m	1990 May 31	3:11:00	26390

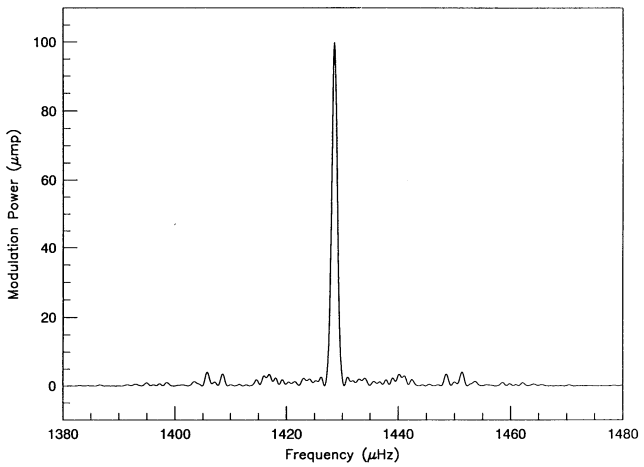

FIG. 2.—Spectral window for the complete GD 358 data set, showing the pattern of peaks that will result from the presence of a single frequency in the power spectrum, in units of micromodulation power (μmp).

taken with two-star or three-star photometers under conditions verified to be photometric by the simultaneous observations of a comparison star, except in South Africa where the second channel was inoperable. Where three channels were available, the third channel kept a continuous record of sky brightness near the target and comparison stars; observers with two channel photometers sampled sky at slightly irregular intervals, as often as deemed necessary by observing conditions. Photon counts from photomultiplier detectors with bialkali (blue-sensitive) photocathodes were accumulated in contiguous 10 s integrations. No filters were used.

Figure 1 shows the central 1 day portion of the light curve for GD 358, when all the participating observatories were online, after sky background and the effects of extinction have been removed. Since our analysis depends primarily on the short-term modulation present, we subtract the mean light level of the star for each run, using the star as its own calibration standard for each telescope, and the individual runs can then be directly combined into a composite light curve in units of fractional intensity.

For this type of analysis we define the unit "modulation intensity" (mi) as a linear representation of the fractional intensity of modulation in the light curves. It is similar to the traditional representation of stellar luminosity in magnitudes, in that 1 mmi ≅ 1 mmag, but it employs a linear rather than a logarithmic scale. We represent the Fourier spectrum derived from the light curves in units of modulation amplitude (ma) or modulation power (mp), which are related in the expected way:

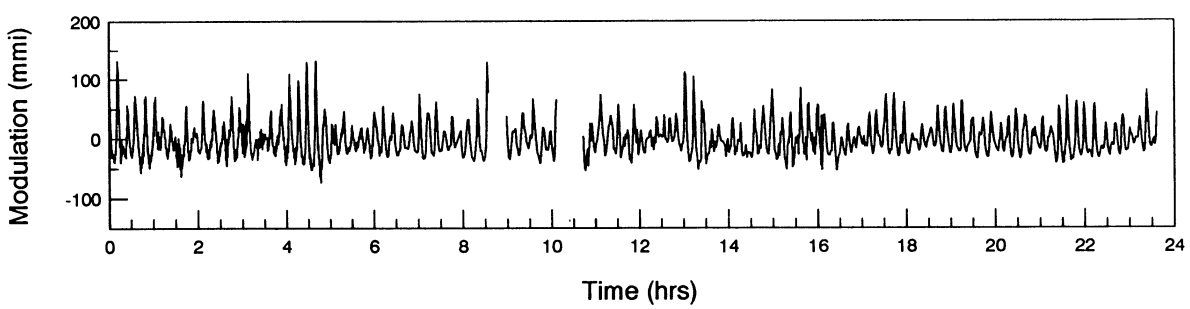

FIG. 1.—Light curve of GD 358 from the central 24 hours of the WET run, after sky effects have been removed and runs from individual telescopes have been combined, in units of millimodulation intensity (mmi).

mp = ma^2. These units allow us to represent the quantities with small integers instead of decimal notation with many leading zeros, or exponential notation where significant differences can be overlooked when they appear in both the number and its exponent. We find that modulation intensities in observed white dwarfs are conveniently expressed in units of mmi, as in Figure 1, and power spectra in units of μmp.

Our coverage is not quite complete, so sometimes there are gaps in the light curve; these gaps produce spectral leakage in the power spectrum—peaks that are artifacts of the data acquisition process and are not astrophysical in origin. We quantify this process by sampling a single, noise-free sine curve in the same manner as the data were sampled, then computing its power spectrum (Nather et al. 1990), which we call the spectral window. It shows the pattern of peaks we can expect to find in the power spectrum were only a single frequency present in our observed light curve (Fig. 2).

The data were nearly continuous during the central portion of the WET run on GD 358; this is demonstrated by the extremely low power levels in the side lobes of the spectral window. This is the best window yet produced by the WET.

3. MODE IDENTIFICATION

We begin our analysis by considering the region of the power spectrum where the power is largest: the region between 1000 and 2400 μHz, shown in Figure 3. The individual stellar pulsations that cause the peaks in the power spectrum are nonradial gravity modes (g-modes). From a theoretical perspective, if we base our models on nonradial gravity modes (g-modes). From a theoretical perspective, if we base our models on nonradial spheroidal modes, we can exploit the strong underlying spherical symmetry, caused by the white dwarf's intense surface gravity, by expanding the pulsation eigenfunctions in terms of spheroidal harmonics $Y_{\ell,m}$. Then there are three quantum numbers which identify a particular mode or eigenfrequency: the degree of the spherical harmonic, ℓ, the azimuthal quantum number, m, and the radial overtone number k. We must first identify unambiguously the degree, ℓ, for each multiplet of frequencies that we will use in constructing our matching model for the star. If we are unable to do this we cannot proceed.

The high-power pulsations in Figure 3 appear in groups of three, with spacings between the groups that increase monotonically with frequency. This is the pattern we expect from a group of multiplets for $\ell = 1$ in a star rotating on its axis, since there can be, at most, $2\ell + 1$ frequencies in an individual multiplet, corresponding to the possible values $m = -1$, $m = 0$, and $m = +1$. For a perfectly spherical star all values of m would have the same frequency, but rotation introduces an asymmetry that causes these frequencies to split apart, so that each value of m will have its own frequency and will be independently represented in the power spectrum. An $\ell = 2$ multiplet can have five members, an $\ell = 3$ can have seven, etc. We find only triplets here, but we must be cautious: it is always possible that only three members of a more complex multiplet are detected.

The multiplets for a given degree should all be about evenly spaced in period, and therefore show progressively wider separation in frequency, corresponding to successive integer values of the radial overtone k. If multiplets of more than one degree are present, as they were in the DOV PG 1159−035 (Winget et al. 1991), then their patterns may overlap each other; they must first be identified with their proper degree before the spacings between multiplets become meaningful.

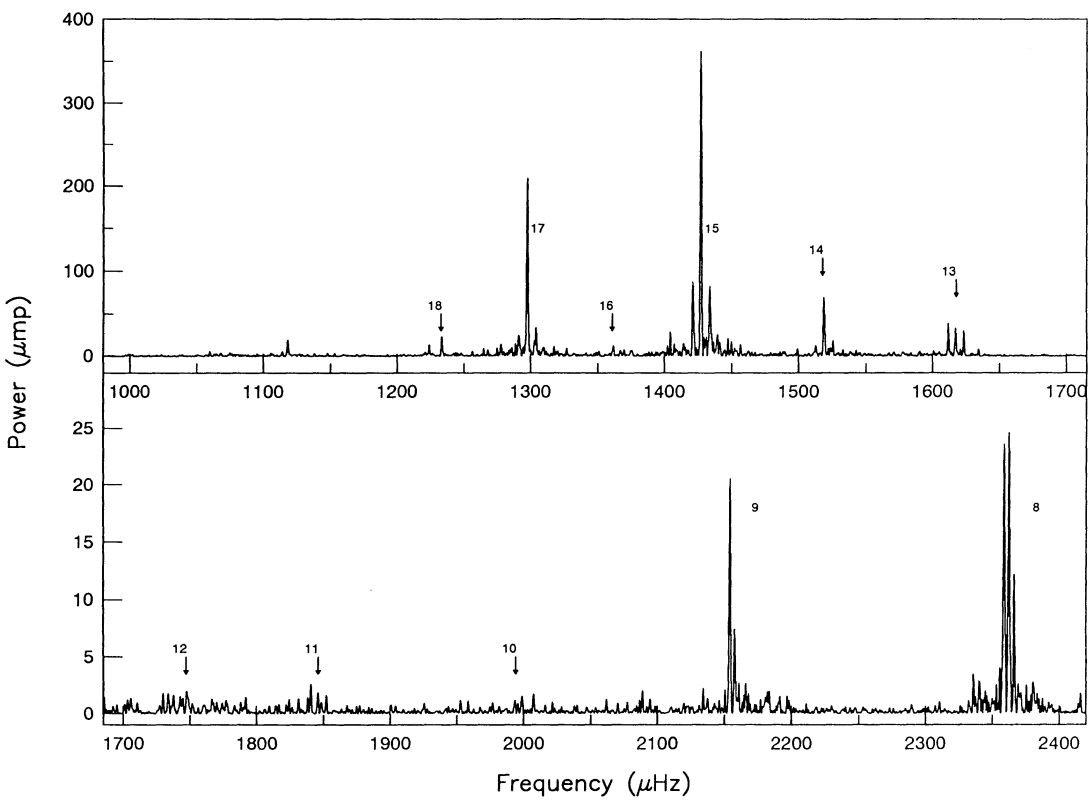

FIG. 3.—Region of highest modulation power in GD 358. The index numbers correspond to the value of the radial overtone (k) for each identified multiplet.

We can explore our spectrum for equal period spacings by first converting it into a "period transform"—showing power as a function of period rather than as a function of frequency—and then taking its Fourier transform to find any preferred spacings in period (the FTPT). We recognize that this is not an ideal procedure: the nonsinusoidal nature of the period transform will yield harmonics in the FTPT that we must identify and disregard, but it has the advantage of being completely objective in its approach. We can also use the Kolmogorov-Smirnov (K-S) test (Kawaler 1988) for the same purpose, but we must first decide which peaks to include; this introduces a subjective element into the process which the FTPT avoids.

Figure 4 (top panel) shows the FTPT for our selected high-power region. The most significant peak appears at 0.0255 Hz, corresponding to a period spacing of 39.2 s, and its (marginally significant) harmonic appears at 0.0510 Hz. We also find a significant peak at 0.0127 Hz, but it arises entirely from the large amplitude of the triplets marked 15 and 17 in Figure 3, and the low amplitude of triplet 16. Its period is about twice 39.2 s and therefore is not an independent spacing. We identify 39.2 s as the period spacing for $\ell = 1$ modes, as exhibited by the separations of the prominent triplets. Then, based on the asymptotic approximation for large values of k, which our models indicate is appropriate for DB pulsators, we would expect $\ell = 2$ multiplets to be spaced at 22.6 s, those for $\ell = 3$ at 16.0 s, and for $\ell = 4$ at 12.4 s.

We find two peaks corresponding to 23.1 and 21.7 s which span our estimate for $\ell = 2$ spacing, and may indicate the presence of these modes at a very low power level. The only other significant peak in the FTPT indicates a spacing of 13.9 s that does not fit our calculated pattern and must arise from some other cause.

The K-S test applied to this spectral region (Fig. 4 lower panel), using all three components of the 10 largest triplets, also shows the 39.2 peak and its harmonic. The same test using only the $m = 0$ components shows the same spacing at lesser significance, and it also shows the 13.9 s spacing found in the FTPT. We identify the 13.9 s spacing as an artifact, brought about by the effects of mode trapping on the individual multiplets—the response of individual modes to the layered structure of the envelope that changes their spacings from each other—which we analyze in detail later. The bifurcation of the significant spacing peaks in the K-S test arises from the same cause. The absence of any spacing near 22 s, which might arise from $\ell = 2$ modes, clearly illustrates the selection effects the K-S test can exhibit: by ignoring the smaller peaks we avoid any noise they might contain, but we may overlook a real spacing that might be imbedded there.

Our identification of both the $\ell = 1$ and $\ell = 2$ modes in PG 1159 was very firm because the ratio of their period spacings had just the expected value, and because the average frequency splitting within each $\ell = 1$ triplet, which arises from the star's

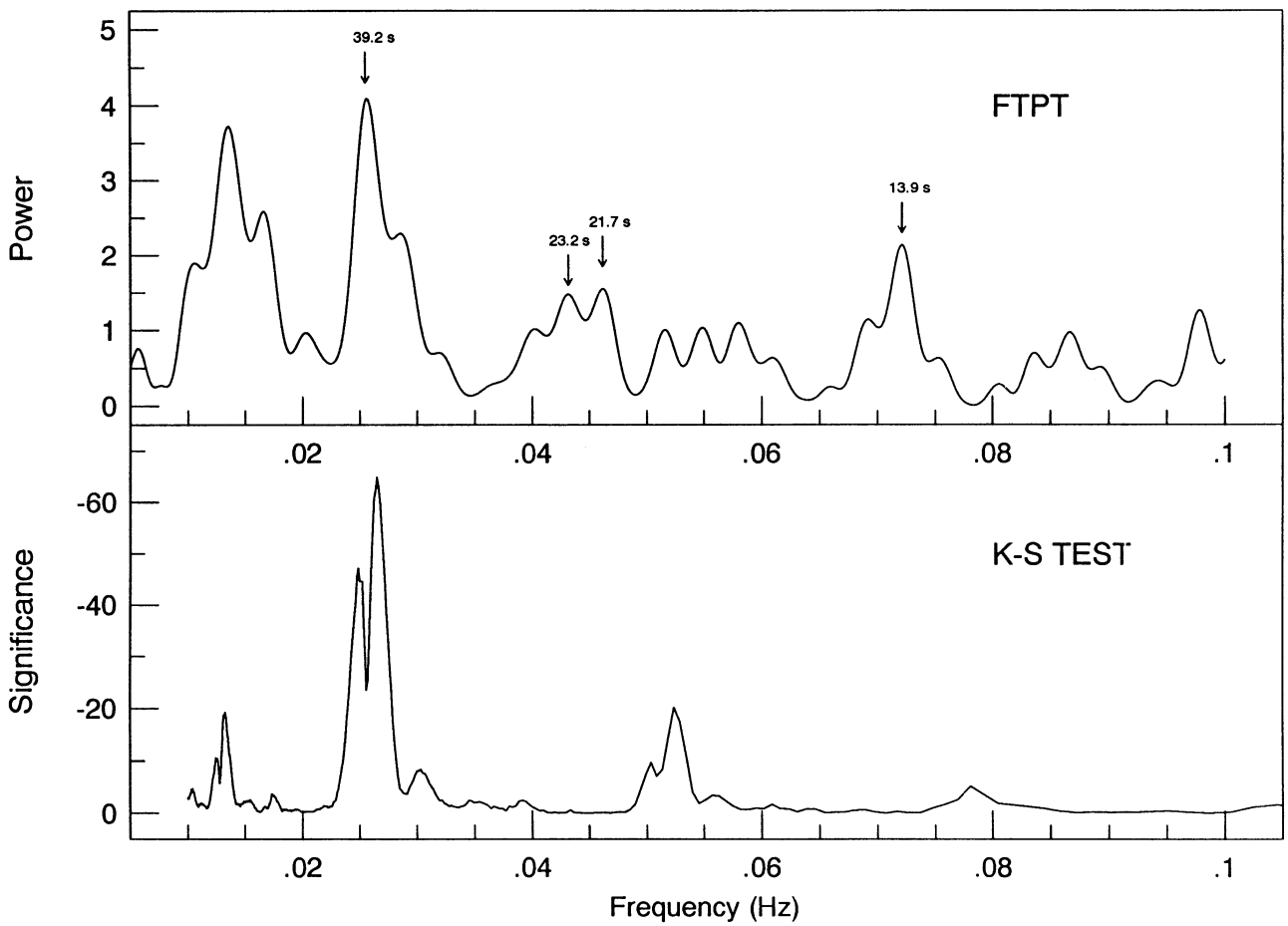

FIG. 4.—Fourier transform of the period spectrum of GD 358 (*upper panel*), confined to the spectral region shown in Fig. 3, and the results of the Kolmogorov-Smirnov test applied to the same region (*lower panel*). Arrows indicate independent period spacings.

rotation on its axis, had the expected ratio with those found in the $\ell = 2$ quintuplets. These frequency splittings were very nearly the same for all the multiplets in PG 1159 so they could be averaged together; they are not the same in GD 358.

Further, we cannot apply this internal check to our identification of the triplets in GD 358 because the very few multiplets we can identify as $\ell = 2$ modes are barely above the noise level in the power spectrum, and some of them overlap, by accident, $\ell = 1$ triplets from which they must be untangled. For example, the spectral region between 2060 and 2100 μHz in Figure 3 shows significant power that cannot be associated with $\ell = 1$, and has peaks with frequency splitting suggesting an $\ell = 2$ quintuplet, but is so low in amplitude and intermixed with measurement noise that the identification is far from certain. If we assume it is an $\ell = 2$ quintuplet, we can locate where other members of its family should fall: they overlap, and therefore may contaminate, the $l = 1$ regions marked 10, 11 and 12, and add power to the aliases on the high-frequency side of 9.

We must therefore rely on external evidence to confirm our triplet identifications as $l = 1$. As we will see, no other identification yields a model that is consistent with all of the observations.

4. ANALYSIS OF THE PERIOD SPACINGS

The mean of the observed period spacings between multiplets for successive values of k provides a measurement of the total mass of the star (Kawaler 1987; Bradley, Winget, & Wood 1993), and the deviations of individual multiplet spacings from their mean yield information about the star's internal structure. Were the object homogeneous, without discontinuities, the period spacing would be nearly uniform. The presence of internal discontinuities—the degeneracy boundary, and the transition regions between different chemical species—cause deviations from uniform spacing that are different for each radial overtone, depending on how it samples the stellar interior. Our analytical procedure is based on synthesis: we construct pulsation models and adjust their parameters until their behavior matches that of the star as nearly as we can magnage it. We then extract these best-fitting parameters, when the fitting process is acceptable, as measurements of the corresponding physical values present in the star.

Figure 5 shows how the individual period spacings dP deviate from their mean, as a function of period (and k-value). We use the mean period spacing to find the nominal period for the $m = 0$ component of each multiplet, then derive dP by subtracting the nominal period from the observed one. We plot as solid dots those deviations where the identification of the central triplet frequency ($m = 0$) is certain, and as hollow dots those points where there could be some ambiguity from measurement noise, or from possibly overlapping $\ell = 2$ modes. An alternative representation of the same information makes use of forward differences ($\Delta P_k = P_{k+1} - P_k$) and is self-normalizing, but each deviation requires that two adjacent modes both be identified and is undefined if they are not. Here we concentrate on the measured mode positions rather than on the intervals between them.

Bradley & Winget (1994), in a companion paper, have explored in detail a series of seismological models designed to match, as nearly as possible, the period spacings found in GD 358. We superpose their best-fitting model spacings (square dots) over the observed spacings in Figure 5. They find that this model has a mass of $0.61 \pm 0.03\ M_\odot$, in good agreement

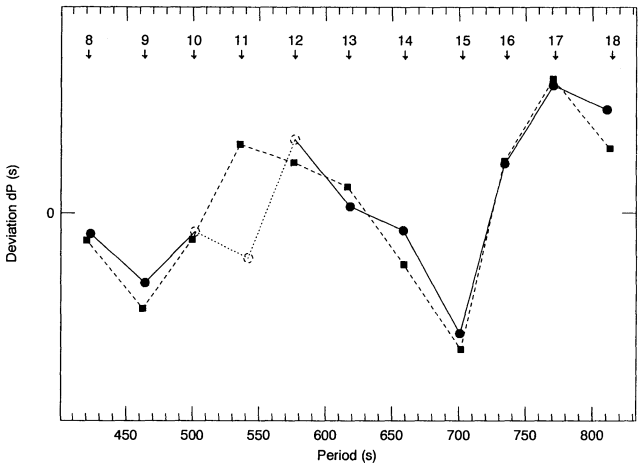

FIG. 5.—Observed deviations of individual periods from their mean (*circles*) and the theoretical model that best fits the data (*squares*). Hollow circles indicate multiplets where the identification of the central frequency peak ($m = 0$) is less certain. The radial overtone number (k) is indicated for each theoretical value.

with a mass of $0.60 \pm 0.17\ M_\odot$ for GD 358 determined by Thejll, Vennes, & Shipman (1991) but somewhat more precise. They also find that the value of k for each triplet is uniquely determined—changing k by ± 1 yields a model that totally fails to fit—so the actual regions of the stellar interior sampled by each radial overtone is known without ambiguity. We use their derived values of k to identify the $\ell = 1$ triplets in our figures.

They further find that fitting the shape of the curve in Figure 5, where the roughly cyclic behavior is caused by the presence of mode trapping, yields a mass for the helium layer, $M_{\rm He} = 2.0 \pm 1.0 \times 10^{-6}\ M_*$, some 10,000 times smaller than the "canonical" value derived from evolutionary models.

They also derive, from their best-fitting model, the absolute luminosity of GD 358 as $0.050 \pm 0.012\ L_\odot$. Combined with a bolometric correction appropriate for an object with the temperature of GD 358 ($24 \pm 1 \times 10^3$ K), they derive a distance of 42 ± 3 pc, in good agreement with the distance derived from measurements of the stellar parallax (Harrington et al. 1985) of 36 ± 4 pc. They find that only the identification of the triplet frequencies in GD 358 as $\ell = 1$ leads to a luminosity, and distance, that agree with the parallax measurements. If they identify them as $\ell = 2$ they derive a distance of ~ 75 pc, and a mass of $0.2\ M_\odot$, totally inconsistent with other measurements of these quantities. If the measured parallax is correct, then the triplets we find must be $\ell = 1$ modes.

5. FREQUENCY SPLITTING WITHIN MULTIPLETS

5.1. *Evidence for Differential Rotation*

In our analysis of PG 1159−035 we found that all of the multiplets for a given ℓ had the same frequency splitting—the absolute value of the difference between the $m = 0$ frequency and that of the other multiplet members—so we could simply averge them together to get a good measurement of their separations, and then derive the rotation period for the star (1.38 ± 0.01 d). This implied that the star was undergoing unifom rotation, at least in those regions sampled by the range of multiplets represented.

GD 358 is not this simple. Its frequency splittings are not constant: they vary with both k and m. Figure 6 shows the measured triplet splittings as a function of k, plotted separately

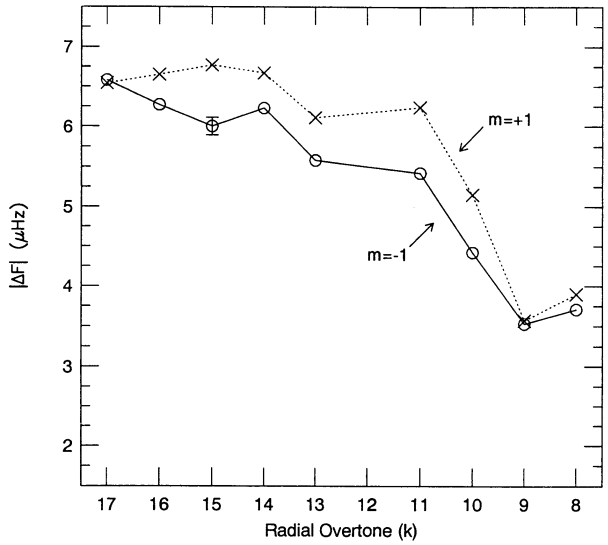

FIG. 6.—Frequency splittings within multiplets, as a function of radial overtone number (k). The greater splittings for larger k-values, which preferentially sample the outer envelope, show the presence of differential rotation. The systematically larger splittings for the $m = +1$ modes than for the $m = -1$ modes show the presence of a weak magnetic field.

for the prograde ($m = +1$) and retrograde ($m = -1$) modes. We immediately notice that the curve has a significant slope, with the smallest frequency splitting (at $k = 8, 9$) some 1.8 times less than the largest (at $k = 16, 17$).

If we identify the triplet structure as caused by stellar rotation, then we must conclude that the star is rotating differentially. The modes of higher k preferentially sample the outer envelope, while those of lower k sample regions closer to the core, and the modes of higher k have significantly larger splittings than those of lower k. The mean splitting of 6.51 μHz for $k = 16, 17$ corresponds to a rotation period of 0.89 d, while the mean splitting of 3.68 μHz for $k = 8, 9$ corresponds to a period of 1.6 d. We conclude that the outer envelope, as sampled by the highest k-values, is rotating 1.8 times faster than that portion of the outer core that is sampled by the smallest k-values we can detect.

5.2. *Evidence for a Magnetic Field*

There is also a significant difference between the frequency splittings associated with the prograde and retrograde modes, although both define a similar overall slope: those associated with $m = +1$ are systematically larger than those for $m = -1$. Following work by Dziembowski & Goode (1984), Jones et al. (1989) described the manner in which rotation and magnetic fields can cause the separation of otherwise degenerate modes into multiplets in white dwarfs. Under the effects of rotation but no magnetic field, the $m = 0$ mode is split symmetrically into $2\ell + 1$ separate frequencies that appear in equal numbers above and below the central frequency, with equal splittings. This is what we found in PG 1159.

In the presence of a weak magnetic field (one which perturbs but does not dominate the motions of the stellar plasma) the modal frequencies are modified in a manner proportional to $|m|^2$, so both outer members of a triplet are increased in frequency with respect to the central frequency. The physical effect involved is straightforward—the presence of the magnetic field "stiffens" the plasma and increases the oscillation frequencies—but the geometry is complex and the detailed calculations are difficult. Nonetheless, we can estimate the strength of a magnetic field that would cause the systematic deviations from symmetrical splitting we have observed, based on the models computed by Jones et al., scaled to considerably lower fields than they considered.

In their Figure 1, they show the frequency splitting between $m = 1$ and $m = 0$ modes for $\ell = 1$, due to the presence of a magnetic field, plotted against the period of the mode. They assumed a dipole field of 10^5 G, but the frequency splitting can be scaled to other field strengths by multiplying by the period of the mode. They assumed a dipole field of 10^5 G, but the frequency splitting can be scaled to other field strengths by multiplying by $B_0^2/(10^5\ \mathrm{G})^2$. For each of the modes in GD 358 with k between 10 and 16 inclusive, we took the measured period and its frequency splitting asymmetry, and calculated the magnetic field required to produce it. This yielded a set of field strengths for these modes with values ranging between 800 and 2000 G. We calculated the error from the dispersion of the values about their mean, choosing 3 σ as a conservative estimate. We consider the simultaneous presence of slow rotation and a weak magnetic field in the Appendix.

From this procedure we calculate the average strength of the magnetic field in GD 358 to be 1300 ± 300 G, a field roughly 1000 times weaker than can be measured from Zeeman splitting of white dwarf spectral lines.

Follow-up observations of GD 358 in 1990 June showed much the same power spectrum as we saw in May, but with two significant differences: the power in the $k = 17$ mode had increased almost 10 times while retaining the same frequency, and the frequency of the $k = 15$ mode had changed by a small but significant 0.5 μHz while its power remained unchanged. Both of these effects suggested the presence of a magnetic field associated with the outer layers of the star, and led to the theoretical exploration of this possibility by Markiel, Thomas, & Van Horn (1994) which has been submitted as a companion paper to this one. Their work suggests that the magnetic field we have found may well be internally generated by the plasma motions associated with pulsation, with convection, or perhaps in the shear region where differential rotation can result in turbulence. The timescale they derive for magnetic field reversal is ~ 2 years, short enough to be consistent with the observed changes. Our observations of GD 358 in 1990 June are still under analysis and will be published elsewhere.

All of the frequencies identified in the 1000–2400 μHz region of the power spectrum, on which we have based our analysis so far, are listed in Table 2.

6. NONLINEAR EFFECTS IN THE POWER SPECTRUM

6.1. *Observations*

When two g-mode pulsations of different frequencies are simultaneously present in the light curve of a luminosity-variable white dwarf, we observe their linear combination as beating—amplitude modulation of the light curve as they come in and out of phase with each other. When there are more than two frequencies present, the process is the same, but the amplitude modulation is more complex, and long strings of data are needed to resolve them if their frequency differences are small. This circumstance was the original motivation for organizing the Whole Earth Telescope observing network.

So long as the medium in which the oscillations propagate can respond in a linear manner, the original frequencies retain

TABLE 2

IDENTIFIED FREQUENCIES FOR $\ell = 1$, 1000–2400 μHz

k	m	Frequency (μHz)	Power (μmp)	|Δ Frequency| (μHz)	Period (s)
17.....	−1	1291.00	24.5	6.58	774.59
	0	1297.58	210.7		770.67
	+1	1304.12	34.1	6.54	766.80
16.....	−1	1355.58	2.4	6.27	737.69
	0	1361.85	12.0		734.30
	+1	1368.50:	7.1	6.65	730.73
15.....	−1	1421.27	87.0	6.00	703.40
	0	1427.27	362.1		700.64
	+1	1434.04	82.4	6.77	697.33
14.....	−1	1512.72	12.6	6.23	661.06
	0	1518.95	69.7		658.35
	+1	1525.62	18.4	6.67	655.47
13.....	−1	1611.80	39.4	5.58	620.42
	0	1617.38	33.4		618.28
	+1	1623.49	29.8	6.11	615.96
12.....	0	1733.88:	1.8		576.76
11.....	−1	1840.46:	2.6	5.42	543.34
	0	1845.88:	1.8		541.75
	+1	1852.12	1.6	6.24	539.92
10.....	−1	1989.26:	0.3	4.42	502.70
	0	1993.68:	1.2		501.59
	+1	1998.83:	1.5	5.15	500.29
9.....	−1	2150.57:	2.1	3.53	464.99
	0	2154.10	20.5		464.23
	+1	2157.67	7.4	3.57	463.46
8.....	−1	2358.85	23.6	3.71	423.94
	0	2362.56	24.8		423.27
	+1	2366.46	12.3	3.90	422.57

all of their original power. When it cannot, however, some of the power is distributed into other frequencies that are the sums and differences of the original frequencies. Communications engineers make use of this property when they design radio receivers: they deliberately introduce a nonlinear element (a "mixer") that creates sums and differences between a local oscillator and the myriad of frequencies that arrive at a radio antenna. A single difference, called the intermediate frequency, is then selected and amplified to provide the output signal. We tune in a particular station by adjusting the local oscillator so its frequency difference matches the receiver's intermediate frequency.

We should not be surprised to find sum and difference frequencies in the resolved power spectrum of a white dwarf's light curve, because the luminosity changes we observe are the effects of changing temperature (Robinson, Kepler, & Nather 1982), and $L \propto T^4$, a distinctly nonlinear transformation. Brassard et al. (1993) have shown that, if this is the only nonlinear process operating, it is possible to estimate how large an effect we should observe and predict the amount of power that should be distributed into combination frequencies.

In Figure 7 we show the full power spectrum of GD 358. Note that the vertical scales are not the same for each panel—we have adjusted them to accommodate the wide range of power in the spectrum. We have labeled 11 triplets in the frequency region between 1000 and 2400 μHz with their k-values, as derived from model fitting by Bradley & Winget (1994). We can identify many peaks above and below this frequency region as combinations; the labels show which k-values combine to form them. These identifications are not exhaustive, so we cannot yet decide if all of the peaks above 2400 μHz are the result of nonlinear combinations, but many of them are. The presence of several multiple combinations is particularly striking: the largest peak in the bottom panel, for example, arises as the triple sum $k = 17 + 15 + 14$. We can find no simple procedure that predicts what amplitude a particular combination frequency will have, but the amount of power in harmonics (the sum of a frequency with itself) is systematically less than in its combination with other frequencies.

The individual frequencies are well enough determined so chance identifications from other possible causes are very unlikely; even so, unambiguous identification can be a complex process. For example, Figure 8 shows an expanded view of the multiplet marked (15 + 13), which seems to have a very odd "hyperfine" structure with it. This is, however, just a result of the straightforward sum of multiplets 15 and 13. The addition of two frequency triplets can create as many as nine different frequencies as their sums; if their frequency splittings are nearly symmetrical, however, only five groups (labeled A–E in Fig. 8) may be resolvable in the spectrum. In this case the frequency splittings in the $k = 13$ and $k = 15$ triplets are sufficiently different, and our resolution high enough, so we can resolve most of them.

Of the nine possible frequencies (k, $m + k$, m) only one (13, −1 +15, −1, labeled A in Fig. 8) is not associated with a significant peak in the spectrum; of the remainder, six correspond closely to the measured frequencies within our measurement error, and two are marginally consistent with them, given the effects of measurement noise and spectral leakage (window effects). The two discordant sum frequencies (in groups B and D) result from the combination of (13, 0) with (15, −1) and (15, +1). Other small discrepancies appear in other combinations as well, often enough to raise the question of the cause, if they are not artifacts. Perhaps some form of magnetic or resonant frequency pulling is at work; if so, the effects are very subtle and difficult to measure. Table 3 shows the combinations we have identified, along with the frequency and power for the largest member of the combination group.

TABLE 3

IDENTIFIED COMBINATION FREQUENCIES FOR $\ell = 1$, 0–5000 μHz

Combination	Frequency (μHz)	Power (μmp)	Combination	Frequency (μHz)	Power (μmp)
15 − 17.....	130.19	10.13	17 + 10	3296.02	0.45
9 − 15.....	726.82	2.98	17 + 9	3451.95	2.13
8 − 14.....	846.21	4.21	15 + 9	3581.47	1.23
8 − 15.....	937.87	2.93	17 + 8	3660.00	1.24
			15 + 8	3789.86	4.14
18 + 17.....	2531.02	2.37	17 + 17 + 17	3892.41	0.73
17 + 17.....	2595.23	3.93	17 + 17 + 16	3958.23	1.22
18 + 15.....	2660.84	5.32	17 + 17 + 15	4022.65	1.77
17 + 15.....	2724.96	18.79	17 + 17 + 14	4114.34	0.32
17 + 14.....	2816.62	3.02	17 + 15 + 15	4152.33	0.62
15 + 15.....	2848.28	3.61	17 + 17 + 13	4211.58	0.71
17 + 13.....	2913.94	2.46	17 + 15 + 14	4244.25	2.41
15 + 14.....	2946.65	19.92	17 + 15 + 13	4342.55	0.56
15 + 13.....	3044.66	4.69	8 + 8	4725.19	0.89
17 + 11.....	3124.38	0.43	17 + 15 + 9	4879.23	0.48

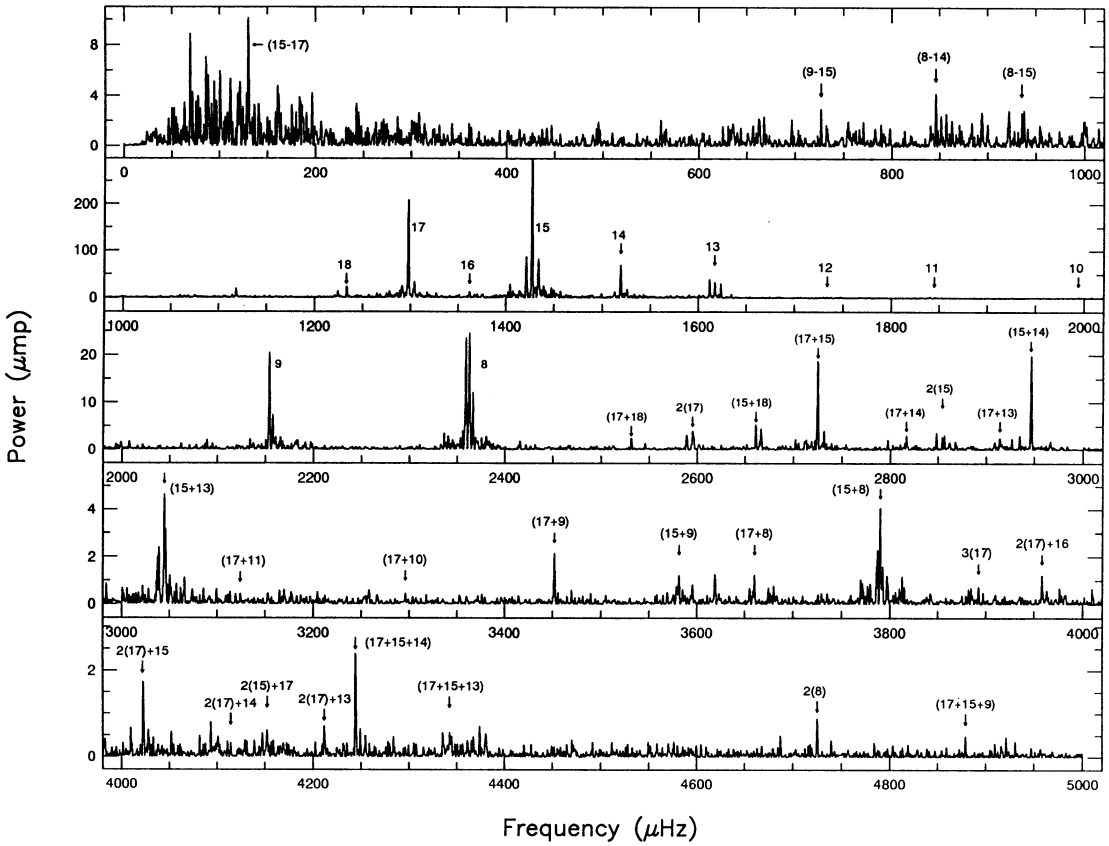

FIG. 7.—Full power spectrum of GD 358. The different scales for each panel attempt to accommodate the large dynamic range present. Triplets are labeled with their corresponding k-value, and the sum and difference frequencies are labeled with the k-values for the triplets which combine to form them.

6.2. *Theory*

In addition to the straightforward process of harmonic distortion—the inability of the propagating medium to respond linearly to the full amplitude of the modulation—the process of resonant mode coupling could also be playing a part here (Dziembowski 1982). Should there exist stable normal modes at (or near) the combination frequencies of active modes, they could be excited to observable amplitude by resonant interaction. We cannot, however, explain the nonlinear effects we see as due to mode coupling, for three reasons:

1. We find too many combination frequencies. The density of normal g-modes decreases with increasing frequency and becomes much too sparse to account for the number of combinations we have found.

2. Harmonic distortion readily describes the details of the observed combinations. The good agreement between the calculated and observed frequency sums for the combination $k = 13 + k = 15$, shown in Figure 8, would be difficult if not impossible to attain using resonant mode coupling as the major cause; the same argument holds for other identified combinations as well.

3. We find too many triple-mode combinations. These would require the unlikely process of higher-order mode coupling to explain, and would result in amplitudes too small to identify above our measurement noise.

We therefore conclude that the nonlinear behavior we observe is caused primarily by harmonic distortion, and that resonant mode coupling alone cannot account for the rich forest of combination frequencies we observe.

The possible effects of harmonic distortion on the temporal spectrum of white dwarfs have already been addressed theoretically by Brickhill (1992) and by Brassard et al. (1993), using somewhat different assumptions about the mechanism

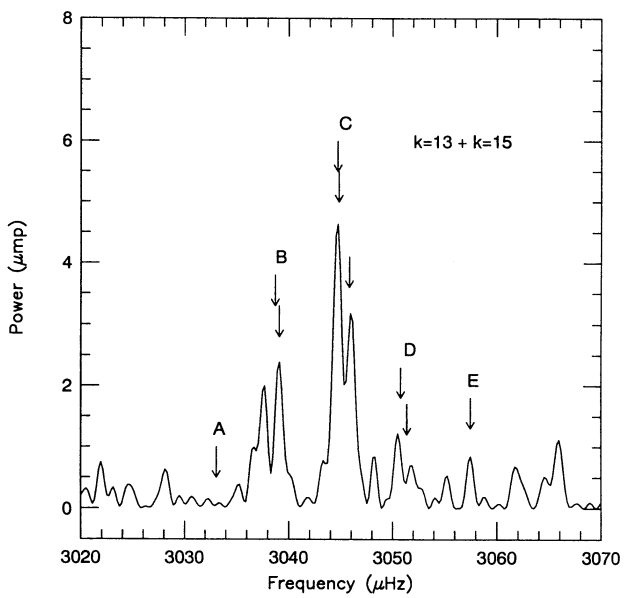

FIG. 8.—Spectral region surrounding the sum of the $k = 13$ and $k = 15$ triplets. Arrows indicate the expected peak locations for the nine possible sum frequencies.

responsible. Brassard et al. assume that the temperature variations are linear (sinusoidal), and that all of the nonlinear behavior results from the transformation to luminosity. If this underlying assumption is correct, then the parameters of an appropriate atmospheric model can be adjusted to yield combination peak amplitudes that match those observed in the star, and can thus provide an independent, seismological measurement of the star's effective surface temperature.

Brickhill presents a model of a DAV pulsator in which pressure variations in the driving region are assumed to be sinusoidal, resulting in temperature variations that are not. This model makes specific predictions about the amplitude of combination frequencies that should appear in the power spectrum as a function of the amplitudes of the parent frequencies. Brickhill's model does not, however, include the effects of the nonlinear transformation to luminosity that forms the core of the work by Brassard et al. We can compare Brickhill's predicted amplitudes with those we observe in GD 358—with the caution that we are comparing an observed DBV object to a model DAV—and find they are systematically much too small. This process alone cannot account for the combination amplitudes we observe, but might contribute to them, and therefore could introduce a systematic error into a seismological measurement of $T_{\rm eff}$.

This is far from an exhaustive list of possible nonlinear effects, but it is clear from the wealth of combination frequencies present that they play an important rôle in the pulsation behavior of many of the variable white dwarfs. We strongly urge theoretical efforts to model this behavior. The success of asterseismology depends on our ability to match these new, high-resolution observations with accurate theoretical descriptions of the processes involved.

7. THE ORIGIN OF GD 358

The population of white dwarfs in the H-R diagram is concentrated along a curve significantly below the main sequence, completely consistent with the view that nuclear fusion is no longer active, and that their further evolution depends only on cooling. The hottest objects associated with this picture are the nuclei of planetary nebulae and the PG 1159 stars, with temperatures in excess of 100,000 K, so hot that the recombination lines of hydrogen are not detectable. Hydrogen lines appear in white dwarf spectra at about 70,000 K, and they dominate their spectra between 45,000 and about 30,000 K: all of the white dwarfs in this temperature region are classified as DA (hydrogen envelope) objects. The helium envelope white dwarfs, with a spectral type DB like GD 358, only appear on the cooling curve at temperatures below 30,000 K.

Vauclair & Fontaine (1979), and Fontaine & Wesemael (1987) have proposed that the DB white dwarfs are, in effect, just mixed-up DA objects: helium convection, which has its onset at about 30,000 K in their models, mixes the thin outer hydrogen layer so thoroughly into the underlying helium that it can no longer be detected in the spectrum. For this to occur the hydrogen layer must be very thin ($\lesssim 10^{-14}\ M_\odot$), and the helium convection zone must be thick enough to completely dilute it. Objects which still have DA spectra below 30,000 K are explained as those that have a hydrogen layer too thick to be "mixed away." As cooling proceeds the convection zone deepens, eventually dredging up material from near the core that brings carbon to the visible stellar surface, explaining the observation of carbon in some DB white dwarfs at 12,700 K and cooler (Pelletier et al. 1986).

Our measurement of the helium layer thickness in GD 358 poses a potential difficulty for this scenario. A helium layer of only $10^{-6}\ M_\odot$ would allow carbon dredge-up to occur at temperatures much higher than are observed, and in far greater abundance than is found. It was an exploration of these models, constrained by the observations of carbon in the cooler white dwarfs, that determined the He layer mass as $10^{-3.5}\ M_\odot$ by allowing it to be a free parameter. It may be difficult to adjust the models to accommodate a layer thickness 300 times smaller. However, the differential rotation we observe in GD 358 could arise as a natural result of cooling and contraction from a DOV object, because its outer envelope will contract far more than its degenerate core, and it must conserve angular momentum while it does so. From the standpoint of rotation, PG 1159 could become a GD 358.

An alternative origin for the DB white dwarfs was suggested by Nather, Robinson, & Stover (1981), who demonstrated that the variable star G61−29 was an interacting pair of degenerate white dwarfs, with helium lines in emission that arise from an accretion disk around the more massive of the pair. They detected no hydrogen in the spectrum, proposing that the mass donor was the remnant of a stellar core in which all of the original hydrogen had been converted to helium, following a model first proposed by Faulkner, Flannery, & Warner (1972). They derived an orbital period of 2800 s from the "S-wave" in the spectrum and proposed that gravitational radiation would force the continued interactive evolution of the system until the mass donor was totally consumed, leaving a single helium-atmosphere white dwarf as a relic.

While it is difficult to argue that the interacting twin-degenerate systems will not become DB white dwarfs, it is also difficult to argue that all DB white dwarfs are formed by this mechanism—the number density of the known objects is too small, and no efficient search technique to find new ones has been devised. The idea is attractive, however, because it can also explain the absence of DB white dwarfs with temperatures above 30,000 K. If they do not descend from hotter single objects, but are formed by the merger process after waiting a long time in "cold storage" as required by the weakness of gravitational radiation that drives them together, then their effective surface temperatures would be established by reheating the outside of a cooler white dwarf. An accretion disk can radiate away far more energy than a contracting white dwarf is able to manage, so a merging system should exhibit a much lower surface temperature. The best-studied twin-degenerate, AM CVn, has an observed temperature near 25,000 K.

The merger model also demands that the relic should have an envelope in rapid rotation, as a result of the deposition of orbital momentum from the consumed companion, in agreement with our findings. The very thin He envelope we have found, however, also poses a problem for any binary-merger model for the origin of GD 358. The model for G61−29, based on the assumption that the mass donor fills its Roche lobe, requires that its mass be about $0.02\ M_\odot$. This amount of He, if transferred to the mass accretor, would yield a much thicker He envelope than we have measured. Further, the measured mass is very close to the mean mass exhibited by single white dwarfs, and we might expect the relic of a merger to have a somewhat larger mass than average. Any detailed merger model would have to address these points.

It is clearly too soon to try to select a model for the process by which GD 358 became a DB white dwarf, but we are encouraged that these new observations, and others to follow, may help guide us to the correct one.

8. SEISMOLOGICAL TECHNIQUES

Temporal spectroscopy—the detailed analysis of the power spectrum of complex, coherent stellar oscillations—allows us to study the internal structure and composition of stars, just as wavelength spectroscopy allows us to study their surfaces. Many of the techniques we use in this analysis are familiar from other types of measurement, while others are unique to stellar seismology; the field is new enough so that technique development still forms an important part of the process.

The identification of low-amplitude peaks in the power spectrum, in the presence of the inevitable noise of measurement, poses a basic problem for this type of analysis. We have found a strong selection criterion in the frequency splitting within an identified multiplet—even where the splittings are unequal, as in GD 358, imposition of a narrow acceptable range of displacements in frequency makes identification much more certain than amplitude criteria alone. We can measure frequency with much greater precision than we can measure amplitude.

In addition to its astrophysical significance, the presence of sum and difference frequencies allows us to assess our errors of measurement in frequency. For example, we measure the $m = 0$ mode for $k = 17$ at 1297.58 μHz and for $k = 15$ at 1427.27 μHz. Their sum is 2724.85 μHz. We measure their sum peak at 2724.96 μHz, so the accumulated measurement error for the three peaks is 0.11 μHz, and the apparent error for the one peak would be $0.11/3^{1/2} = 0.06$ μHz. By accumulating these individual errors from the sum peaks we can identify, we estimate our average rms error as ± 0.11 μHz for any one frequency measurement.

The presence of nonlinear effects also offers an interesting observational possibility: the detection of high-degree modal patterns not expected to be visible to us. We view the whole of the stellar disk because we cannot resolve it spatially, so the observable amplitude of modes $\ell \gtrsim 3$ is reduced by geometric cancellation effects (Dziembowski 1977) if they are sinusoidal. If they are not, however, geometric cancellation will be far less effective, and we may be able to detect them if they are present, or be able to set useful limits if we cannot.

9. SUMMARY AND CONCLUSIONS

We summarize first the results concerning the pulsation properties of GD 358 that our observations have revealed:

1. As in PG 1159, we find evidence for pulsations of degree $\ell = 1$ and $\ell = 2$, but no evidence that higher degree pulsations are excited to detectable amplitudes. In GD 358 all the large amplitude modes have $\ell = 1$; the multiplets with $\ell = 2$ are too small to be useful in our analysis.

2. The amplitudes vary with m within and between multiplets, as they do in PG 1159, but not in any pattern we are able to understand. Mysteries remain.

3. The values for the radial overtone number k for each multiplet are uniquely determined by detailed model fitting, so the regions of the interior they sample are known without ambiguity.

4. The absolute luminosity is also determined to high accuracy, and is a sensitive function of the degree assigned to the pulsations. Model fitting can therefore identify ℓ by demanding that its apparent distance agree with that obtained from stellar parallax measurements.

5. The rich pattern of sum and difference frequencies we observe shows that nonlinear effects are important, but rules out resonant mode coupling as a major cause. Resonance may have some perturbing effect on the measured combination frequencies, however.

We next summarize our results concerning the stellar physics of GD 358:

1. Differential rotation is evident in the star, based on the trend of frequency splitting as a function of the radial overtone number, k. The outer envelope is rotating 1.8 times faster than the core.

2. The systematic deviations from symmetrical frequency splitting for modes with $m = -1$ and $m = +1$ provide strong evidence for the presence of a magnetic field. We estimate its strength at 1300 ± 300 G. Theoretical work by Van Horn et al. finds a plausible explanation for this field as self-generated, by a dynamo process.

3. The rich spectrum of observed sum and difference frequencies, many involving triple combinations, indicate that nonlinear effects are significant in GD 358. The largest pulsations have harmonics with amplitudes significantly less than those of their combined sums, suggesting the nonlinearity arises in the regions through which the pulsations propagate, rather than where they are driven.

4. The mass of GD 358 is 0.61 ± 0.03 $M_\odot$, derived from detailed model fitting to the deviations from uniform triplet period spacing.

5. The best-fitting model measures the helium layer thickness as $M_{\rm He} = 2.0 \pm 1.0 \times 10^{-6}$ M_*. If this value is typical for DB stars it provides a strong and important contraint on their evolutionary origin.

6. The absolute luminosity of GD 358 is 0.050 ± 0.012 $L_\odot$, derived from detailed model fitting.

7. The seismological distance to GD 358 is 42 ± 3 pc, based on its derived absolute luminosity, and assuming a bolometric correction appropriate to a star with its $T_{\rm eff}$ of $24 \pm 1 \times 10^3$ K. The distance derived from parallax measurements is 36 ± 4 pc.

The theory and practice of stellar seismology continues to surprise us with the richness and detail of its scientific return. We have limited our main analysis of GD 358 to the small, high-amplitude region of the total power spectrum, with minimal exploration of the remainder. This star, and others like it, still have much to teach us about their structure and their history, and temporal spectroscopy offers us an effective way to study them.

We thank Pawel Moskalik and Wojtek Dziembowski for helpful discussions. This work was supported in part by a PYI award, AST-8552457, to D. E. W. by the National Science Foundation. P. B. acknowledges financial support by the NSERC Canada and by the Fund FCAR (Québec). P. A. B. acknowledges a Continuing Education Fellowship during 1990–1991. M. C. and P. B. acknowledge support from the Government of Western Australia through the Department of State Services, and they thank Lowell Observatory for the use of the 24 inch reflector and Arie Verveer for technical support. We also thank Arlo Landolt for the loan of the LSU two-channel photometer that was used in Hawaii.

APPENDIX

Following the analysis of, for example, Jones et al. (1989), we can develop expressions for the change in the pulsation frequency due to the presence of slow rotation, and weak magnetic fields. Both physical effects break the azimuthal symmetry and thereby the m-degeneracy of modes with the same radial quantum number, k, and degree, ℓ. This can produce fine structure similar to that observed in many pulsating white dwarf stars (see the discussions in Winget et al. 1991, and Jones et al. 1989).

The key to differentiating between the two distinct effects is the number of components resulting in the fine-structure multiplet: rotation produces $2\ell + 1$ components, and fields of the sort considered by Jones et al. produce only $\ell + 1$ components. Both the above cited sets of authors point out that simply counting multiplet components can be used as an empirical test to distinguish between the effects.

Of perhaps greater astrophysical interest is the circumstance when both physical effects are simultaneously present in a star. We assume, following Jones et al., that the magnetic and rotation axes are aligned. We further assume that the rotation rates and the magnetic field strengths are small; then if we regard the effects on frequencies and eigenfunctions as operators, the rotation operator and the magnetic operator commute. That is to say, the corrections are linear. Then the order in which one computes the frequency changes is unimportant and the final frequency distribution is given by:

$$\sigma_{k,\ell,m} = \sigma_{k,\ell} + m\,\delta\sigma_{\rm rot} + |m|^2\,\delta\sigma_B\,.$$

Then the splitting terms can be determined from the observed frequencies using the following expressions:

$$\delta\sigma_{\rm rot} = \frac{\sigma_{m=+1} - \sigma_{m=-1}}{2}$$

and

$$\delta\sigma_B = \sigma_{m=+1} - \delta\sigma_{\rm rot} - \sigma_{m=0}\,,$$

or, rewriting using the formula for $\delta\sigma_{\rm rot}$,

$$\delta\sigma_B = \frac{(\sigma_{m=+1} + \sigma_{m=-1})}{2} - \sigma_{m=0}\,.$$

Note that when $\delta\sigma_{\rm rot} \gg \delta\sigma_B$, the identification of the $m = \pm 1$ and $m = 0$ is unambiguous. This is the case for GD 358. We also ignore, for this purpose, the effect of the magnetic field on the mode for $m = 0$, which cannot be determined directly from the observed frequencies, and must be smaller than $\delta\sigma_B$. Then from the above expressions we can estimate the rotation rate and the magnetic field strength using the results of Jones et al.

REFERENCES

Bradley, P. A., & Winget, D. E. 1994, ApJ, 430, 850
Bradley, P. A., Winget, D. E., & Wood, M. A. 1993, ApJ, 406, 661
Brassard, P., Fontaine, G., Wesemael, F., & Talon, A. 1993, in White Dwarfs: Advances in Observations and Theory, ed. M. A. Barstow (Dordrecht: Kluwer), 485
Brickhill, A. J. 1992, MNRAS, 259, 529
Dziembowski, W. 1977, Acta Astron., 27, 203
———. 1982, Acta Astron., 32, 147
Dziembowski, W., & Goode, P. R. 1984, Mem. Soc. Astron. Ital., 55, 185
Faulkner, J., Flannery, B. P., & Warner, B. 1972, ApJ, 175, L79
Fontaine, G., & Wesemael, F. 1987, in IAU Colloq. 95, 2d Conf. on Faint Blue Stars, ed. A. G. D. Philip, D. S. Hayes, & J. Liebert (Schenectady: Davis), 319
Harrington, R. S., et al. 1985, AJ, 90, 123
Iben, I., Jr., & Reinzini, A. 1983, ARA&A, 21, 271
Jones, P. W., Pesnell, W. D., Hansen, C. J., & Kawaler, S. D. 1989, ApJ, 336, 403
Kawaler, S. D. 1987, in Stellar Pulsations, ed. A. N. Cox, W. M. Sparks, & S. G. Starrfield (Berlin: Springer), 367
———. 1988, in IAU Symp. 123, Advances in Helio- and Asteroseismology, ed. J. Christensen-Dalsgard & S. Fransden (Dordrecht: Reidel), 329
McGraw, J. T. 1977, Ph.D. thesis, Univ. Texas
Markiel, J. A. Thomas, J. H., & Van Horn, H. M. 1994, ApJ, 430, 834
Nather, R. E., Robinson, E. L., & Stover, R. J. 1981, ApJ, 244, 269
Nather, R. E., Winget, D. E., Clemens, J. C., Hansen, C. J., & Hine, B. P. 1990, ApJ, 361, 309
Pelletier, C., Fontaine, G., Wesemael, F., Michaud, G., & Wegner, G. 1986, ApJ, 307, 242
Robinson, E. L., Kepler, S. O., & Nather, R. E. 1982, ApJ, 259, 219
Thejll, P., Vennes, S., & Shipman, H. L. 1991, ApJ, 370, 355
Vauclair, G., & Fontaine, G. 1979, ApJ, 230, 563
Winget, D. E. 1988, in IAU Symp. 123, Advances in Helio- and Asteroseismology, ed. J. Christensen-Dalsgaard & S. Frandsen (Dordrecht: Reidel), 305
Winget, D. E., Hansen, C. J., Liebert, J., Van Horn, H. M., Fontaine, G., Nather, R. E., Kepler, S. O., & Lamb, D. Q. 1987, ApJ, 315, L77
Winget, D. E., et al. 1991, ApJ, 378, 326
Wood, M. A. 1992, ApJ, 386, 539